

A constitutive model for concrete confined by steel reinforcement and carbon fiber reinforced plastic sheet

Yeou-Fong Li[†]

Department of Civil Engineering, National Taipei University of Technology, No. 1, Sec. 3,
Chung-Hsiao E. Rd., Taipei, 106-08, Taiwan, R.O.C.

Tsang-Sheng Fang[‡]

Department of Civil Engineering, National Taiwan University, Taiwan, R.O.C.

(Received April 9, 2003, Accepted January 19, 2004)

Abstract. In this paper, we modify the L-L model (Li *et al.* 2003) and extend the application of this model to concrete confined by both steel reinforcement and CFRP. Thirty-six concrete cylinders with a dimension of $\phi 30 \times 60$ cm were tested to verify the effectiveness of the proposed model. The experimental test results show that different types of steel reinforcement have a great effect on the compressive strength of concrete cylinders confined by steel reinforcement, but the different types of steel reinforcement have very little effect on concrete cylinders confined by both steel reinforcement and CFRP. Compared with the stress-strain curves of confined concrete cylinders, we can conclude that the proposed model can provide more effective prediction than others models.

Key words: carbon fiber reinforced plastics; steel reinforcement; constitutive model; confined concrete.

1. Introduction

Column is the most important structural member, and its strength and ductility affect the seismic performance of the structure significantly. Therefore, the seismic retrofit of columns has become a very important issue in the areas sitting on an earthquake zone. Although retrofiting materials and methods have been developed for a long time, CFRP composite material applied to seismic retrofit projects became a very popular method in the last decade. The carbon fiber reinforced plastic sheet is wrapped around the column to increase the compressive strength, shear strength and ductility of the column. In the early retrofit design, most of the compressive strength models of the confined concrete only consider the increased strength provided by CFRP, while the increased strength provided by steel reinforcement was usually neglected. However, in existing structures, the column members usually contain lateral steel reinforcement. In this paper, the proposed model was verified

[†] Professor

[‡] Graduate Student

by using the stress-strain relationships of thirty-six concrete cylinders with three different types of steel reinforcements (circular hoop, circular lap spliced hoop, and spiral) confined by CFRP. In the meantime, the proposed model and the Mander model were used to compare the stress-strain curves of the experimental results of concrete confined by steel reinforcement. Also, the proposed model and Kawashima model were used to compare the stress-strain curves of the experimental results of concrete confined by steel reinforcement and CFRP together.

2. Literature review

Confined concrete constitutive models have been researched extensively since the early 20th century. The following paragraphs introduce chronologically some popular stress-strain constitutive models for confined concrete. Some of the peak strength prediction formulas for concrete confined by steel reinforcement are listed in Table 1.

Considire (1903) was the first researcher to propose that adding spiral steel reinforcement in concrete columns can increase their strength and ductility. Richart *et al.* (1929) proposed that the uni-axial strength of confined concrete is the unconfined concrete strength plus a linear function of the lateral confinement stress provided by the spiral reinforcement, shown in Table 1. Later, Balmer (1949) and Newman *et al.* (1971) modified the coefficient of Richart's model, shown in Table 1. Kent and Park (1971) proposed a second-order parabola for the ascending branch and a linear descending branch. Park *et al.* (1982) modified the Kent and Park's stress-strain model by adding the effect of the unconfined concrete stress and introducing the increase of the concrete strength due to lateral confinement. Muguruma *et al.* (1980) proposed a model of two second-order parabolas stress-strain curves. Sheikh *et al.* (1980, 1982) proposed a stress-strain model in which the peak stress is a function of the effective confining stress, which is the confinement effectiveness coefficient times the confining stress. In Sheikh's model, the confinement effectiveness coefficient depends on the configuration of the hoop reinforcement. Ahmad and Shah (1982) studied the relationship between the spiral spacing, spiral amount, and the confinement stress. The proposed stress equation for confined concrete is the function of unconfined concrete strength and lateral confinement stress. Mander *et al.* (1988a, 1988b) then modified the confined peak stress and

Table 1 The peak strength prediction formulas for concrete confined by steel reinforcement

Previous study	Peak strength of confined concrete
Richart <i>et al.</i> (1928)	$f'_{cc} = f'_c + 4.1 \times f'_l$
Balmer (1949)	$f'_{cc} = f'_c + k_1 \times f'_l$, where $k_1 = 4.5 \sim 7.0$
Newman <i>et al.</i> (1971)	$f'_{cc} = f'_c + 3.7 (f'_l / f'_c)^{-0.14} \times f'_l$
Mander <i>et al.</i> (1988)	$f'_{cc} = f'_c \left(-1.254 + 2.254 \sqrt{1 + \frac{7.94 f'_l}{f'_{co}}} - 2 \frac{f'_l}{f'_c} \right)$
Saatcioglu <i>et al.</i> (1992)	$f'_{cc} = f'_c + 6.7 (f'_l)^{-0.17} \times f'_l$
Hoshikuma <i>et al.</i> (1997)	$f'_{cc} = f'_c + 3.8 \times f'_l$
Mirmiran <i>et al.</i> (1997)	$f'_{cc} = f'_c + 4.269 \times f'_l^{0.587}$

proposed a functional expression to represent the stress-strain curve. The confinement effectiveness coefficient of the Mander's model for circular, square, and wall-type sections was introduced based on a theory proposed by Sheikh *et al.* (1982). Fujii *et al.* (1988) proposed a model consisting of a second-order parabola and a third-order curve for the ascending branch stress-strain curve. Saatcioglu and Razvi (1992, 1999) proposed a parabolic ascending branch followed by a linear descending branch for the stress-strain curve and a confinement model for high-strength concrete using the equations proposed by Mander *et al.* (1988). Kawashima *et al.* (1997, 1998, and 1999) proposed a series of stress-strain models for concrete confined by steel reinforcement, CFRP, and both steel reinforcement and CFRP. In the constitutive model of concrete confined by steel reinforcement proposed in 1997, the ascending branch was idealized by an n^{th} -order polynomial equation. Then, Kawashima *et al.* used the regression analysis of experimental results and modified the above-mentioned 1997's model to extend the application to different confinement materials by adjusting the coefficients. The model for concrete confined with both steel reinforcement and CFRP proposed by Kawashima *et al.* (1999) will be called the Kawashima model in this paper. Mirmiran and Shahawy (1997) proposed an equation to predict the peak strength for glassy fiber reinforced plastics (GFRP) based on test results of 30 concrete cylinders with a dimension of $\phi 15 \times 30$ cm. Li *et al.* (2003) proposed an effective constitutive model for concrete confined with CFRP. More details about this model will be discussed in the next section. Lam *et al.* (2001) proposed a model that appears to be the first one that recognizes explicitly the effect of the type of FRP. Xiao *et al.* (2001) used more than two hundred concrete stub columns with nine different types of FRP jackets and proposed a constitutive model for confined concrete. Karabinis *et al.* (2001) found that the external reinforcement of concrete by CFRP sheet can effectively enhance the strength and ductility of concrete as well as energy absorption even in low volumetric ratios. Wang *et al.* (2001) proposed that even though the steel reinforcement has little influence on the strength of concrete but its contribution should not be neglected when the steel reinforcement spacing reduces.

3. Constitutive model

The confined concrete constitutive model (named L-L model) proposed by Li *et al.* (2003) was originally developed for concrete confined by CFRP. In this paper, we modify the L-L model and extend the application of this model to concrete cylinders confined, respectively, by steel reinforcement only, by CFRP only, and by steel reinforcement and CFRP together. In the proposed model, the equation of the lateral confining stress due to steel reinforcement was adopted from Mander model (1988) and the equation of the lateral confining stress due to CFRP was adopted from the L-L model, respectively. In this section, the ascending branch stress-strain curve of the proposed model for concrete confined by both steel reinforcement and CFRP will be introduced in details. Fig. 1 is the illustration of steel reinforcement and CFRP confining concrete cylinder.

Because the mechanism of confined concrete is similar to the mechanism of soil under tri-axial loading, the stress relation of confined concrete can be derived from tri-axial stress relation. According to the Mohr-Columb failure envelope of the soil under later confined stress (σ_3), the axial stress (σ_1) could be expressed as follows:

$$\sigma_1 = 2c \tan(45^\circ + \phi/2) + \sigma_3 \tan^2(45^\circ + \phi/2) \quad (1)$$

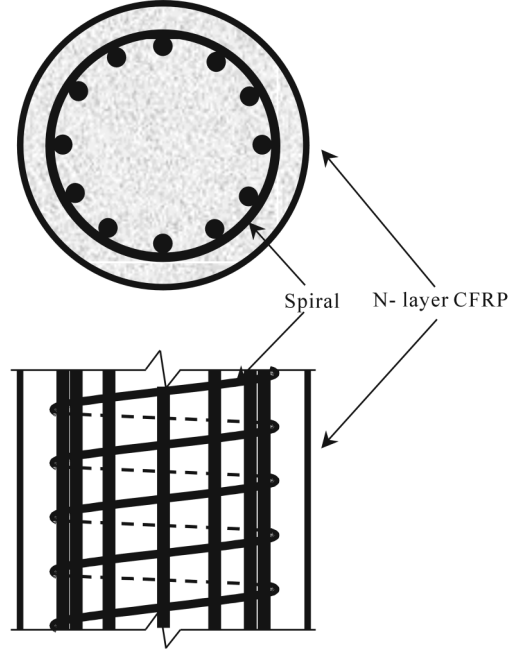


Fig. 1 The illustration of steel reinforcement and CFRP confining concrete cylinder

In Eq. (1), σ_1 is the axial stress, c is the cohesion of the soil or rock, σ_3 is the lateral confined stress, and ϕ is the angle of internal friction of material. If Eq. (1) is the tri-axial stress relation equation of confined concrete, then σ_3 is the effective confined stress and $f'_l = \sigma_3$, while σ_1 is the maximum axial strength and $f'_{cc} = \sigma_1$. When $\sigma_3 = 0$ (i.e., the unconfined situation), the plain concrete strength can be expressed as $\sigma_1 = 2c \tan(45^\circ + \phi/2) = f'_c$. By using the above physical-based constitutive model for confined concrete, the compressive strength of confined concrete (f'_{cc}) can be calculated as follow:

$$f'_{cc} = f'_c + f'_l \times \tan^2\left(45^\circ + \frac{\phi}{2}\right) \quad (2)$$

In Eq. (2), f'_c is the compressive strength of the unconfined concrete and f'_l is the effective lateral confining strength. In the case of the effective lateral confining strength come from the lateral steel reinforcement and CFRP together. We assume that the uni-axial force is uniformly distributed inside the concrete cylinder. When the uni-axial loading was applied, the CFRP and lateral steel reinforcement started to resist the uni-axial compressive force simultaneously. Inside the core of the concrete cylinder, the lateral confining stress comes from the lateral steel reinforcement and the CFRP can be added together. The peak axial compressive strength of the proposed model can be written as follows:

$$f'_{cc} = f'_c + (f'_{l1} + f'_{l2}) \times \tan^2\left(45^\circ + \frac{\phi}{2}\right) \quad (3)$$

In the above equation, f'_{cc} is the peak compressive strength of the confined concrete, f'_c is the compressive strength of the unconfined concrete, f'_{l1} is the effective lateral confining strength provided by the lateral steel reinforcement, and f'_{l2} is the effective lateral confining strength provided by CFRP composite material. Since the ultimate strain of CFRP is usually greater than 1.0%, and it is greater than the yielding strain of steel reinforcement, we can use the yielding stress as the stress to calculate the confining stress provided by steel reinforcement. In Eq. (3), f'_{l1} , f'_{l2} , and ϕ can be represented as follows:

$$f'_{l1} = \frac{1}{2}k_e\rho_s f_{yh} \quad (\text{From Mander's model}) \quad (4)$$

$$f'_{l2} = \frac{2 \times k_c \times n \times t \times E_{cf} \times \varepsilon_{cf}}{D} \quad (5)$$

$$\phi = 36^\circ + 1^\circ \times \left(\frac{f'_c}{35} \right) \leq 45^\circ \quad (6)$$

In Eq. (4), f'_{l1} is the effective lateral confining strength due to steel reinforcement, k_e is the confinement effectiveness coefficient, and k_e depends on the type of lateral steel reinforcement, shown as follows:

$$k_e = \frac{A_e}{A_{cc}} = \frac{\left(1 - \frac{s'}{2d_s}\right)^2}{1 - \rho_{cc}} \quad (\text{For circular hoop}) \quad (7)$$

$$k_e = \frac{1 - \frac{s'}{2d_s}}{1 - \rho_{cc}} \quad (\text{For circular spiral}) \quad (8)$$

Also in Eq. (4), ρ_s is the ratio of the volume of transverse confining steel to the volume of confined concrete core, and f_{yh} is the yield strength of the transverse reinforcement.

In Eq. (5), k_c is the coefficient of section shape (Priestley *et al.* 1996), n is the jacket layer of CFRP, t is the thickness of CFRP per layer, E_{cf} is the elastic modulus of CFRP, D is the diameter of the cylinder, and ε_{cf} is the ultimate strain of CFRP.

In Eq. (6), ϕ is the angle of internal friction of concrete, which is in proportion with the compressive strength of concrete, and usually varies from 36° to 45° (Goodman 1989). The angle of internal friction “ ϕ ” can be expressed as a function of concrete strength (Li *et al.* 2003) as shown in Eq. (6).

In Eq. (7), A_e is the area of the effectively confined core concrete, A_{cc} is the area of the core of column section within center lines of perimeter spiral, s' is the clear spacing between spiral or hoop bars, d_s is the diameter of spiral, and ρ_{cc} is the ratio of the area of axial steel to the area of the core of section.

When the axial stress reaches the peak axial compressive strength “ f'_{cc} ”, the CFRP breaks and its strain reaches the ultimate strain ε'_{cc} . For the compatibility condition of concrete cylinder and CFRP deformation, the ultimate strain is mainly controlled by the strength of CFRP composite materials. Therefore, ε'_{cc} can be expressed as the following equation:

$$\varepsilon'_{cc} = \varepsilon'_c \left[1 + \alpha \tan^2 \left(45^\circ + \frac{\phi}{2} \right) \frac{f'_{l2}}{f'_c} \right] \quad (9)$$

In Eq. (9), ε'_c is the strain at the compressive strength of the unconfined concrete (f'_c), usually set at $\varepsilon'_c = 0.002$. Parameter “ α ” is related to the material properties of confinement material; α equals to 2.24 (Li *et al.* 2003) in this paper and its corresponding CFRP material properties are listed in Table 2.

Table 2 Material properties of CFRP

Material specification	FAW 200 (g/m ²)
Young's modulus, E_{cf}	230,535 MPa (2.35×10^6 kgf/cm ²)
Tensile strength	4120.2 MPa (42000 kgf/cm ²)
Thickness	0.011 cm/layer
Ultimate strain	0.018

As the strain “ ε_c ” falls between 0 to ε'_{cc} , the ascending branch stress-strain relation of the proposed model can be simulated by using the third-order polynomial equation, as shown in Eq. (10).

$$f_c = a\varepsilon_c^2 + b\varepsilon_c + c \quad (10)$$

And, the corresponding three boundary conditions are shown as follows:

$$f_c = 0 \quad (\text{at } \varepsilon_c = 0) \quad (11)$$

$$f_c = f'_{cc} \quad (\text{at } \varepsilon_c = \varepsilon'_{cc}) \quad (12)$$

$$df_c/d\varepsilon_c = 0 \quad (\text{at } \varepsilon_c = \varepsilon'_{cc}) \quad (13)$$

In this paper, the proposed stress-strain relationship of the constitutive model is only valid for the strain range from 0 to ε'_{cc} . As the CFRP fracture and the strain just over ε'_{cc} , the stress drop tremendously. Therefore, the slope at the peak is a discontinuous function. We choose the boundary shown in Eq. (13) to obtain the stress-strain relationship is a good approximation.

In the case of the effective lateral confining strength come from the lateral steel reinforcement and CFRP together. We assume that the uni-axial force is uniformly distributed inside the concrete cylinder. When the uni-axial loading was applied, the CFRP and lateral steel reinforcement started to resist the uni-axial compressive force simultaneously. Inside the core of the concrete cylinder, the lateral confining stress comes from the lateral steel reinforcement and the CFRP can be added together. Upon substituting the boundary conditions into Eq. (10), the stress-strain relation of confined concrete are shown as follows:

$$f_c = f'_{cc} \left[-\left(\frac{\varepsilon_c}{\varepsilon'_{cc}} \right)^2 + 2\left(\frac{\varepsilon_c}{\varepsilon'_{cc}} \right) \right] \quad (0 \leq \varepsilon_c \leq \varepsilon'_{cc}) \quad (14)$$

where f'_{cc} and ε'_{cc} are calculated from Eq. (2) and Eq. (9).

4. Experimental program

Thirty-six concrete cylinders with a dimension of $\phi 30 \times 60$ cm were designed and tested to verify the effectiveness of the proposed model. In this section, the design and fabrication of concrete cylinders and related uni-axial test programs will be introduced.

4.1 Design of concrete cylinders

These thirty-six concrete cylinders were divided into 4 groups, and each group was applied with nil, 1, and 2 layers of CFRP composite material. For each design parameter, three concrete cylinders were needed. Groups A, B, C, and D represent different types of steel reinforcement, such as circular hoop, two C-shaped lap-splice hoops, circular spiral, and without steel reinforcement, respectively. The illustration configuration of the concrete cylinder is shown in Fig. 2.

Table 3 introduces the naming principles of the thirty-six concrete cylinders. The first letter means the type of steel reinforcement. "A" means circular hoop, "B" means two C-shaped lap-splice hoops, "C" means circular spiral, and "D" means no steel reinforcement. The number following the first letter means the number of layers of CFRP applied on the concrete cylinder. The second number means the serial number of the concrete cylinder. For example, "A-1-2" represents the specimen confined by circular hoop with 1-layer CFRP, and its serial number is 2.

The designed concrete strength is 17.2 MPa (175 kgf/cm²), and the designed concrete slump is 12 cm. The steel reinforcement used in the concrete cylinders is No. 3, and its yield strength is 274.7 MPa.

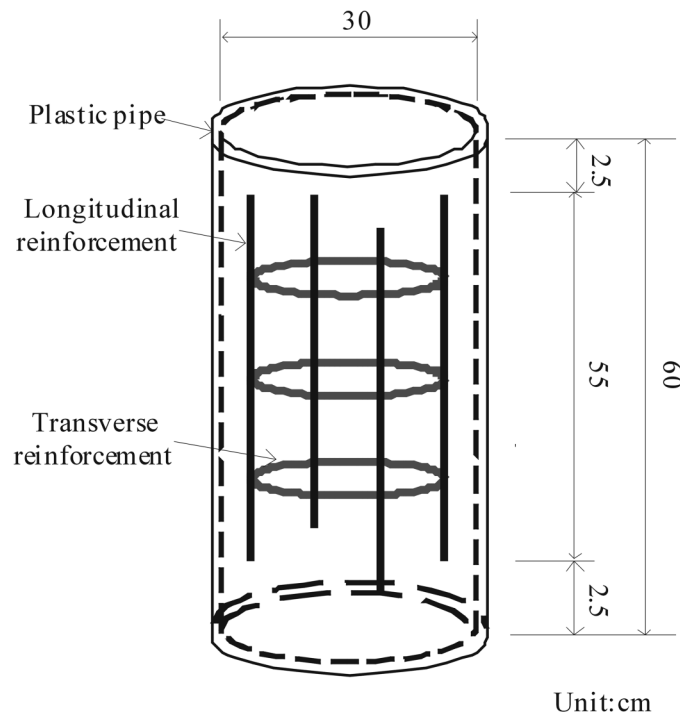


Fig. 2 The illustration configurations of the concrete cylinder

Table 3 The naming of concrete cylinders

Group	Specimens	CFRP layers	Type of steel reinforcement
A	A-0	0	Circular hoop
	A-1	1	
	A-2	2	
B	B-0	0	Lap-splice
	B-1	1	
	B-2	2	
C	C-0	0	Spiral
	C-1	1	
	C-2	2	
D	D-0	0	Nil
	D-1	1	
	D-2	2	

The spacing of the steel reinforcement is 10 cm, and the concrete cover thickness is 2.5 cm. For the circular hoop and two C-shaped lap-splice hoops, the lap length of steel reinforcement is 11.5 cm. The longitudinal rebars are used to hold the horizontal steel reinforcements in position. A total of thirty-six plastic pipes, with an internal diameter of 30 cm and a height of 60 cm, are used as the formworks of the concrete cylinders. Premixed concrete is used in the experiment.

4.2 The procedures of wrapping CFRP

The hand-applying procedures are as follows. A thin layer of primer epoxy was first applied to the concrete surface. After the primer epoxy on the concrete surface was cured at the ambient temperature for several hours, the carbon fiber sheet was applied to the concrete cylinders. For each layer of carbon fiber sheet, two plies of epoxy, one on the cylinder surface prior to installing the sheet and the other on top of the installed sheet, were applied using a paintbrush to fully saturate the carbon fiber with epoxy. The extra epoxy for each layer was squeezed out using a flat plastic scraper. After the required sheet of layers was applied, the CFRP jacketing was cured in the ambient condition. The length of overlay is more than 10 cm, and the duration before applying the next layer should be more than one day. After the required sheet of layers was applied, the CFRP jacket as cured in the ambient condition.

4.3 Instrumentation of the compression test

This test program was undertaken by the 4900 kN (500 tf) universal-testing machine, which is load controlled, at the structural laboratory of the National Taipei University of Technology. The experimental equipment includes a load cell, a linear voltage displacement transformer, an analog/digital converter with a signal amplifier, and a personal computer.

In order to make sure that the uni-axial force was applied uniformly on the top and bottom surfaces of the concrete cylinder, the two surfaces were paved horizontally with gypsum. The

loading rate of the actuator is 3.5 (kgf/cm²)/sec, and the loading process was stopped when the axial load began to decrease.

4.4 Experimental observations

The failure mode of the concrete cylinders confined by CFRP is similar to that of the conical shape. The failure mechanism of cylinders confined by steel reinforcement and 2-layer CFRP is described as follows. The concrete between CFRP and steel reinforcement was spalling, and the CFRP was broken in the center of the cylinder. This shows that the concrete inside the steel reinforcement was still confined by steel reinforcement when the CFRP was broken.

The experimental observations of the rest of the specimens confined with CFRP and with/without

Table 4 The peak strengths and their corresponding strains of the experimental results

Group	Specimens	Average f'_{cc} MPa (kgf/cm ²)	Average ϵ'_{cc}
A	A-0	17.96 (183.10)	0.0026
	A-1	32.27 (328.94)	0.0051
	A-2	39.89 (406.58)	0.0061
B	B-0	18.42 (187.76)	0.0021
	B-1	31.85 (324.62)	0.0042
	B-2	40.90 (416.94)	0.0073
C	C-0	20.05 (204.43)	0.0025
	C-1	33.13 (337.74)	0.0041
	C-2	39.87 (406.45)	0.0063
D	D-0	16.68 (170.03)	0.0019
	D-1	25.52 (260.11)	0.0042
	D-2	33.64 (342.88)	0.0067

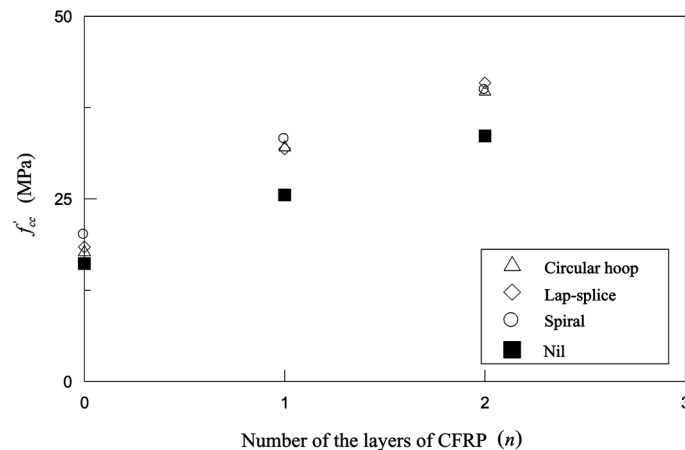


Fig. 3 The relationships of the average peak compressive strengths of confined concrete and numbers of layers of CFRP

steel reinforcement are described as follows. When the stress of the actuator reached the peak strength of the confined concrete, the breaking sound of broken CFRP was heard continuously, and then the CFRP broke in the middle of the cylinder and also the concrete crashed. The breaking position of the CFRP was not necessarily at the overlaying position.

The measured peak strengths f'_{cc} and their corresponding strains ϵ'_{cc} are listed in Table 4. As seen from the experimental results in Table 4, we can obtain that the experimental results between each specimen have a small relative error; and this indicates that the quality of the specimens is very stable. The relationships of the average peak compressive strength of confined concrete and the number of layers of CFRP are drawn in Fig. 3. As seen from Fig. 3, we can obtain the following conclusions:

1. When concrete cylinder is confined by steel reinforcement (Groups A, B, and C), its compressive strength is higher than those without steel reinforcement (Group D) and the compressive strength is highly dependent on the types of steel reinforcement. The compressive strength due to spiral increases larger than that due to 2-C-shaped lap-splice and circular hoop.
2. When concrete cylinders are confined by steel reinforcement and CFRP together (Groups A, B, and C), their compressive strengths are very close to each other. This indicates that the compressive strength of concrete cylinders confined by CFRP was irrelevant to the types of steel reinforcement. The reason is that when CFRP reaches its ultimate strain (usually 0.015), the strains of steel reinforcement of Groups A, B, and C are still within yielding strain and ultimate strain. The stresses of steel reinforcement of Groups A, B, and C are all at the yielding stress. Therefore, the confinement stresses due to steel reinforcement of Groups A, B, and C are the same, and Eq. (4) and Eq. (5) are both reasonable equations.

5. Discussion on the theoretical/experimental results

In this section, the theoretical (calculated from different models) and experimental results of the peak strength of confined concrete, the strain at the peak strength, and the stress-strain curve are compared. Due to the difference and complexity of the confinement materials, the comparisons of the experiment results and the models are divided into three categories, listed in Table 5.

5.1 The comparison of the peak strength

5.1.1 The proposed model

The peak strengths of Group D specimens are compared with the peak strengths calculated by the

Table 5 Experimental specimens vs. constitutive models for different confinement conditions

Confinement	Specimens	Constitutive models
Nil, or CFRP	D-0, D-1, D-2	Proposed model
Steel reinforcement	A-0, C-0	Proposed model and Mander
Steel reinforcement and CFRP	A-1, A-2 B-1, B-2 C-1, C-2	Proposed model and Kawashima

Table 6 Error analyses of the peak strengths of the proposed model

Specimens	Experiment MPa (kgf/cm ²)	Proposed model MPa (kgf/cm ²)	Error (%)
D-0	16.68 (170.03)	16.68 (170.03)	0
D-1	25.52 (260.11)	25.90 (263.97)	1.5
D-2	33.64 (342.88)	35.11 (357.94)	4.4
Average absolute error (%) =			2.95

Table 7 Error analyses of the peak strengths of the proposed model and Mander models

Specimens	Experiment MPa (kgf/cm ²)	Proposed model MPa (kgf/cm ²)	Error (%)	Mander MPa (kgf/cm ²)	Error (%)
A-0	17.96 (183.10)	21.60 (220.17)	20.3	22.91 (233.56)	27.6
C-0	20.05 (204.43)	22.64 (230.76)	12.9	24.04 (245.09)	19.9
Average absolute error (%) =		16.6		23.8	

proposed model, and the error analysis of the peak strengths are listed in Table 6. Since the unconfined concrete strength is the peak strength of the specimens, the average error of the D-0 specimens is zero. As for D-1 and D-2 specimens, the errors are 1.5% and 4.4% respectively. The average error of the proposed model is 2.95%. The proposed model can predict the peak strengths of concrete confined by CFRP very well.

5.1.2 The proposed model and the Mander model

The Mander model was originally proposed for concrete confined by steel reinforcement. The peak strengths of A-0 and C-0 specimen series are compared with the peak strengths calculated by the proposed model and Mander model, and the error analysis of the peak strengths are listed in Table 7. As seen in Table 7, the average absolute errors of the Modified and Mander models are 16.6% and 23.8% respectively, and the proposed model is more accurate than the Mander model in predicting the peak strength.

5.1.3 The proposed model and the Kawashima model

In the last century, most of the confined constitutive models were proposed specifically for concrete columns confined by either steel reinforcement or CFRP. Not until 1999 did Kawashima *et al.* (1999) propose a constitutive model for concrete confined by both steel reinforcement and CFRP*W

The peak strengths of A-1, A-2, B-1, B-2, C-1, and C-2 specimens are compared with the peak strengths calculated by the proposed model and the Kawashima model, and the error analysis of the peak strengths are listed in Table 8. As seen in Table 8, the average absolute errors of the proposed model and the Kawashima model are 2.8% and 10.1% respectively. We can conclude that the

*In the papers by Kawashima *et al.* (1997, 1998, 1999), the diameter to height ratio of the circular cylinder (column) is 1:3. But, the diameter to height ratio of the circular concrete cylinder used in this paper is 1:2. Therefore, we justify the peak strength proposed by the Kawashima model by raising it 8%.

Table 8 Error analyses of the peak strengths of the proposed model and Kawashima models

Specimen	Experiment MPa (kgf/cm ²)	Proposed model MPa (kgf/cm ²)	Error (%)	Kawashima MPa (kgf/cm ²)	Error (%)
A-1	32.27 (328.94)	30.82 (314.15)	-4.5	35.35 (360.35)	9.5
A-2	39.89 (406.58)	40.04 (408.12)	0.4	44.70 (455.63)	12.1
B-1	31.85 (324.62)	30.82 (314.15)	-3.2	35.35 (360.35)	11.0
B-2	40.90 (416.94)	40.04 (408.12)	-2.1	44.70 (455.63)	9.3
C-1	33.13 (337.74)	31.86 (324.73)	-3.8	35.35 (360.35)	6.7
C-2	39.87 (406.45)	41.08 (418.71)	3.0	44.70 (455.63)	12.1
Average absolute error (%) =		2.8		10.1	

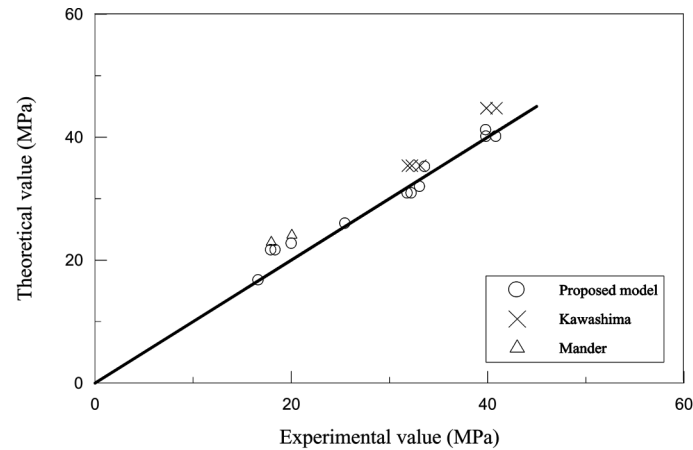


Fig. 4 The comparison between the peak strengths calculated by Mander, Kawashima, proposed model models and the experimental results

proposed model is more accurate than the Kawashima model in predicting the peak strength.

As seen in Fig. 4, the peak strengths calculated by the Mander and Kawashima models overestimate the experimental results, while the peak strengths calculated by the proposed model can predict the experimental result very well.

5.2 The comparison of the strain at peak strength

5.2.1 The proposed model

The strains at the peak strengths of specimen Group D are compared with the strain at the peak strengths calculated by the proposed model. The average errors of D-0, D-1, and D-2 specimens are 5.3%, 7.1% and 4.5% respectively. The average error of the proposed model is 5.6%.

5.2.2 The proposed and the Mander models

The strains at the peak strengths of A-0 and C-0 specimens are compared with the strains at the peak strengths calculated by the proposed model and the Mander model. The average absolute

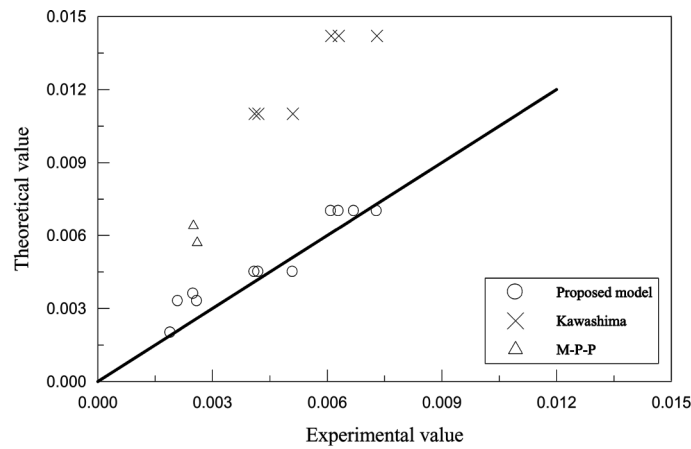


Fig. 5 The comparison between the strains at the peak strengths calculated by Mander, Kawashima, proposed model models and the experimental results

errors of the Modified and Mander models are 5.9% and 137.6% respectively. The proposed model is more accurate than the Mander model in predicting the strain at the peak strength.

5.2.3 The proposed model and the Kawashima model

The strains at the peak strengths of A-1, A-2, B-1, B-2, C-1, and C-2 specimens are compared with the strains at the peak strengths calculated by the proposed model and the Kawashima model. The absolute maximum errors of the proposed model and the Kawashima model are 7.4% and 95.8%. We can conclude that the proposed model is more accurate than the Kawashima model in predicting the strain at the peak strength.

As seen in Fig. 5, the strains at the peak strengths calculated by the Mander and Kawashima models overestimate the experimental results, while those calculated by the proposed model can predict the experimental result very well.

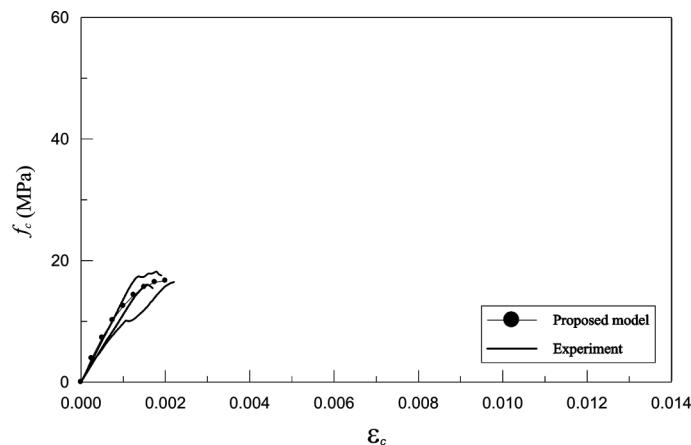


Fig. 6 The stress-strain curves of D-0 specimens and the proposed model

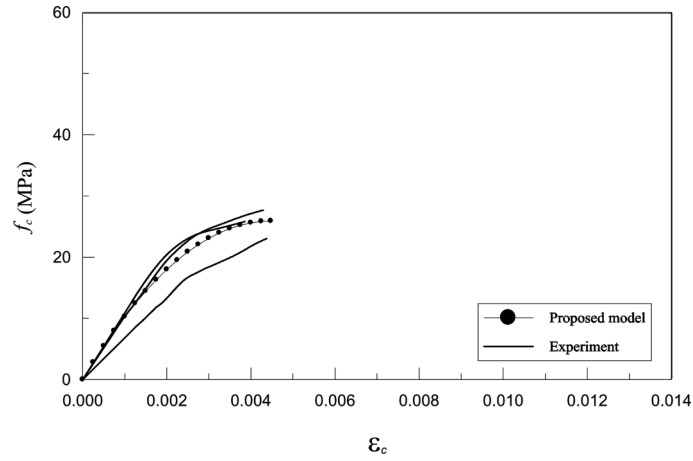


Fig. 7 The stress-strain curves of D-1 specimens and the proposed model

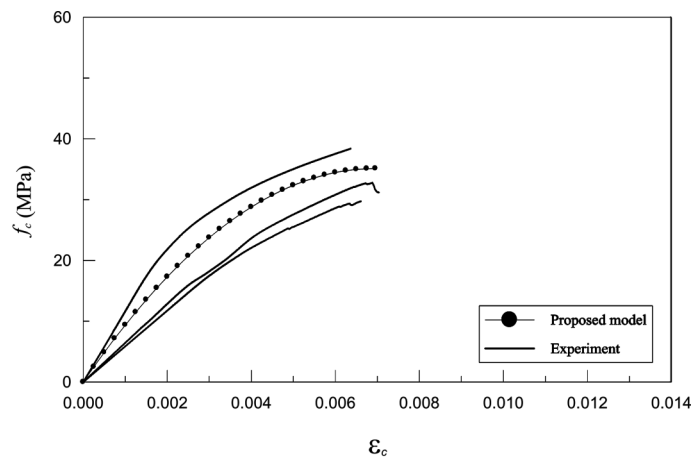


Fig. 8 The stress-strain curves of D-2 specimens and the proposed model

5.3 The comparison of the stress-strain curve

5.3.1 The proposed model

The stress-strain curves of the experiment results of D-0, D-1, and D-2 specimens are compared with the stress-strain curves calculated by the proposed model, shown in Fig. 6, Fig. 7, and Fig. 8, respectively. As seen in the above figures, we can conclude that the proposed model can simulate the experimental results very well.

5.3.2 The proposed model and the Mander model

The stress-strain curves of the experiment results of the A-0 and C-0 specimens, and the proposed model and the Mander model are plotted in Fig. 9, and Fig. 10, respectively. As seen in the above figures, the peak strength " f'_{cc} " of Mander's model is close to that of the proposed

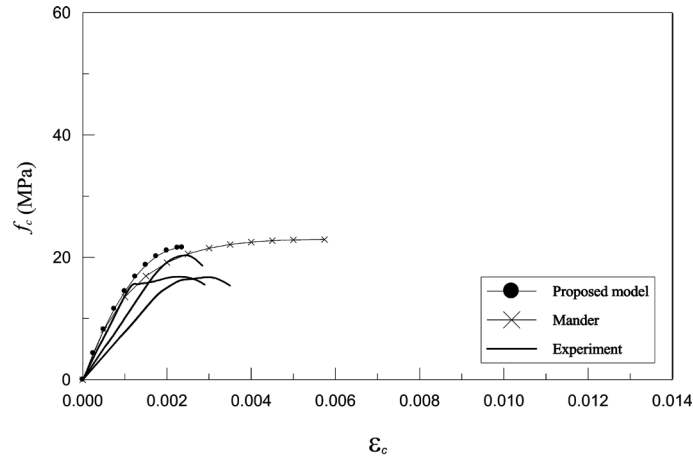


Fig. 9 The stress-strain curves of A-0 specimens, the Mander, and the proposed models

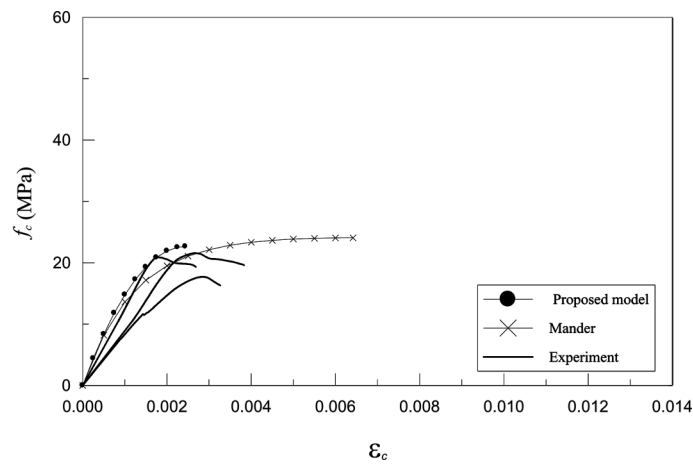


Fig. 10 The stress-strain curves of C-0 specimens, the Mander, and the proposed models

model; but the strain “ ε_{cc}' ” at peak strength is much larger than that of the proposed model. We can conclude that the proposed model simulates the experimental results better than the Mander model.

5.3.3 The proposed model and the Kawashima model

The stress-strain curves of the experiment results of the A-1, B-1 and C-1 specimens, and the proposed model and the Kawashima model are shown in Fig. 11~Fig. 13 respectively. Similarly, the stress-strain curves of the experimental results of the A-2, B-2 and C-2 specimens, and the proposed model and the Kawashima model are shown in Fig. 14~Fig. 16 respectively. As seen in Fig. 11~Fig. 16, the stress-strain curves of the proposed model can fit the experimental stress-strain curves very well. As for the Kawashima model, the prediction of stress is acceptable, but the prediction of strain is greatly overestimated.

From the observations and discussions on the experimental results of stress-strain curves among

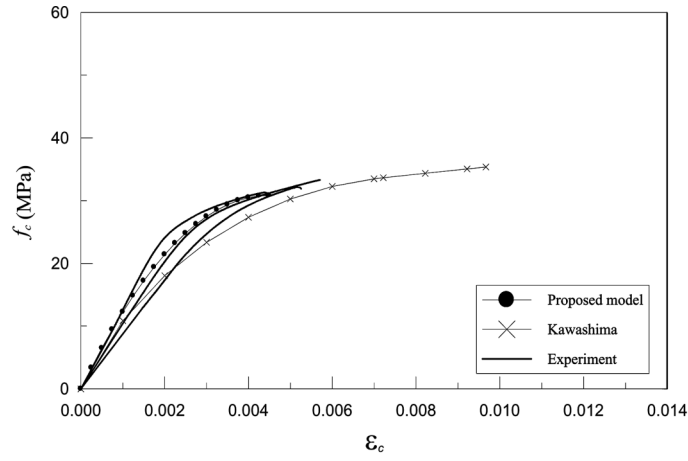


Fig. 11 The stress-strain curves of A-1 specimens, the Kawashima, and the proposed models

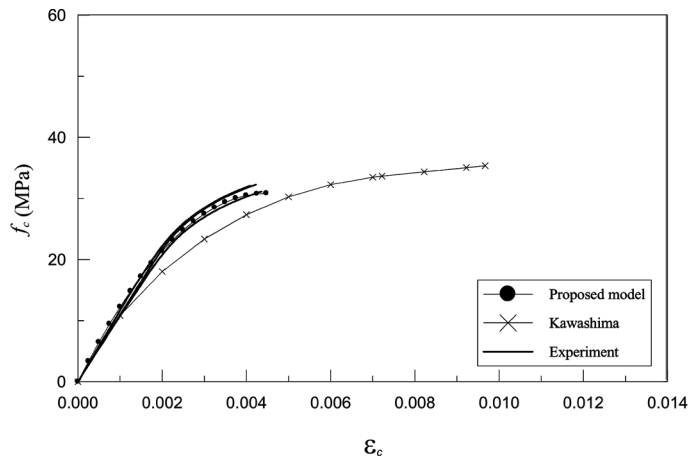


Fig. 12 The stress-strain curves of B-1 specimens, the Kawashima, and the proposed models

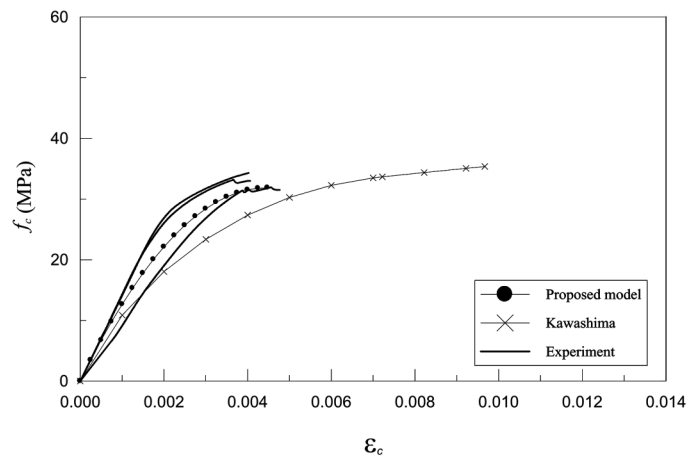


Fig. 13 The stress-strain curves of C-1 specimens, the Kawashima, and the proposed models

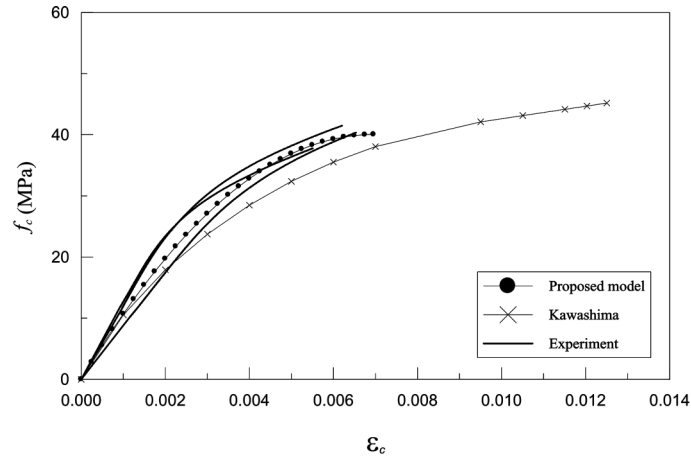


Fig. 14 The stress-strain curves of A-2 specimens, the Kawashima, and the proposed models

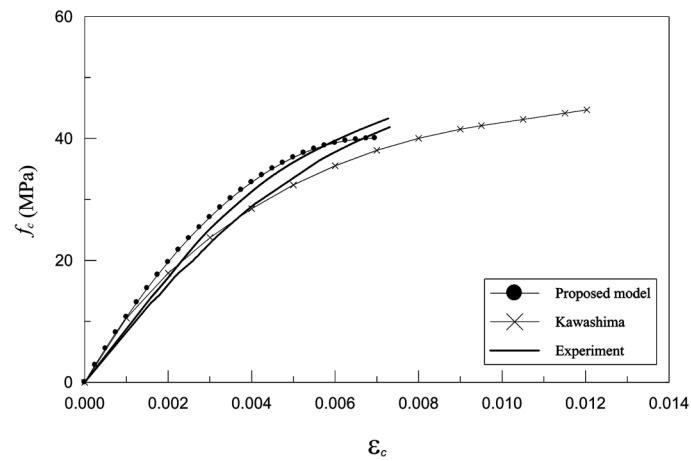


Fig. 15 The stress-strain curves of B-2 specimens, the Kawashima, and the proposed models

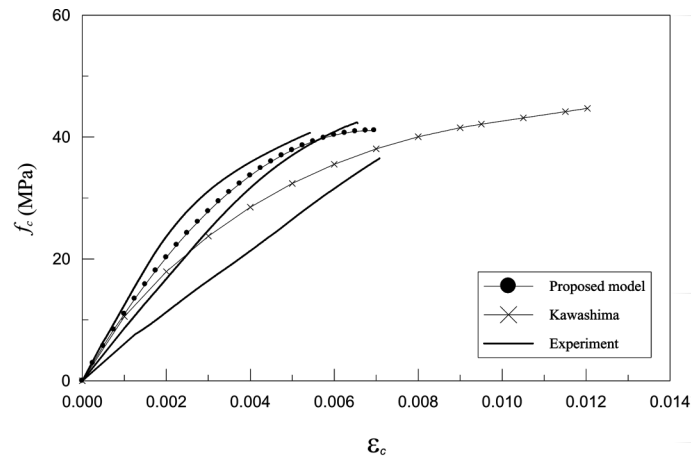


Fig. 16 The stress-strain curves of C-2 specimens, the Kawashima, and the proposed models

the three models, we can conclude that the proposed model is more effective than the Mander and Kawashima models in the prediction of the peak stress, strain at the peak stress, and the stress-strain curves.

6. Conclusions

From the observation of the experimental results and by comparing the experimental results to the constitutive models, we can arrive at the following conclusions:

1. The peak stress formula of the proposed model is a theoretical equation, and it is derived from the Mohr-Columb failure envelope theory, which conforms to the fundamental theory of plasticity. The formula can be used in different levels of confining stress.
2. When concrete cylinders are confined by different types of steel reinforcement, the compressive strength is highly dependent on the types of steel reinforcement.
3. When concrete cylinders are confined by CFRP and different types of steel reinforcement, their compressive strengths are very close to each other. This indicates that the compressive strength of concrete cylinder confined by CFRP is irrelevant to the types of steel reinforcement.
4. Compared to the test results of the 36 concrete cylinders, the average absolute errors of the peak strength estimation of the proposed model are less than 3%, with the exclusion of the cylinders confined by steel reinforcement only (such as the A-0, and C-0 series). As for Mander's and Kawashima's models, their average absolute errors are about 20%. Also the average absolute errors of the strain at the peak strength of the proposed model are less than 8%. As for Mander's and Kawashima's models, their average absolute errors are much larger than that of proposed model.
5. Comparing the stress-strain curves of the experimental results with those of the proposed, Mander's, and Kawashima's models, we can conclude that the proposed model is more effective than Mander's and Kawashima's models.
6. The proposed model can be applied to concrete cylinders confined by steel reinforcement only, by CFRP only, and by both steel reinforcement and CFRP.

Acknowledgements

The authors would like to thank Mr. C.-C. Fang for his support in helping to make the concrete cylinders. The valuable comments of Prof. C.-C. Chern at National Taiwan University is also greatly appreciated.

References

- Ahmad, S.H. and Shah, S.P. (1986), "Orthotropic model of concrete for tri-axial stresses", *J. Struct. Eng.*, ASCE, **112**, 165-181.
- Balmer, G.G. (1949), "Shearing strength of concrete under high tri-axial stress-computation of Mohr's envelope as a curve", Structural Research Laboratory Report No. SP-23, U.S. Bureau of Reclamation.
- Caltrans (1994), *The Northridge Earthquake-Post Earthquake Investigation Report*, Division of Structures, Caltrans.

- Considire, A. (1903), *Experimental Researches Reinforced Concrete*, L.F. Moisseiff, translator, McGraw-Hill, New York.
- Fujii, M. and Kobayashi, K. (1978), "A study on the application of a stress-strain relation of confined concrete", *Proceedings, JCA Cement and Concrete*, Japan Cement Association, Tokyo, Japan, **42**, 429-432.
- Goodman, R.E. (1989), *Introduction to Rock Mechanics*, John Wiley & Sons, N.Y.
- Hognestad, E. (1951), "A study of combined bending and axial load in reinforced concrete members", Engineering Experimental Station, University of Illinois, Bulletin Series No. 399.
- Hoshikuma, J., Kawashima, K., Nagaya, K. and Taylor, A.W. (1997), "Stress-strain model for confined reinforced concrete in bridge piers", *J. Struct. Eng.*, ASCE, **123**, 624-633.
- Hosotani, M., Kawashima, K. and Hoshikuma, J. (1998), "A stress-strain model for concrete cylinders confined by carbon fiber sheets", *Civil Engineering*, JSCE, **39**(592), 37-52. (in Japanese)
- Hosotani, M. and Kawashima, K. (1999), "A stress-strain model for concrete cylinders confined by both carbon fiber sheets and hoop reinforcement", *Civil Engineering*, JSCE, **43**(620), 25-42. (in Japanese)
- Karabinis, A.I. and Rousakis, T.C. (2001), "Carbon F.R.P. confined concrete elements under axial load", *FRP Composite in Civil Engineering*, CICE, 309-316.
- Kent, D.C. and Park, R. (1971), "Flexural members with confined concrete", *J. Struct. Div.*, ASCE, **97**, 1969-1990.
- Lam, L. and Teng, J.G. (2001), "A new stress-strain model for FRP-confined concrete", *FRP Composite in Civil Engineering*, CICE, 283-292.
- Li, Y.-F., Lin, C.-T. and Sung, Y.-Y. (2003), "A constitutive model for concrete confined with carbon fiber reinforced plastics", *Mechanics of Materials*, **35**, 603-619.
- Maguruma, H., Watanabe, S. and Tanaka, S. (1978), "A stress-strain model of confined concrete", *Proc., JCA Cement and Concrete*, Japan Cement Association, Tokyo, Japan, **34**, 429-432.
- Mander, J.B., Priestley, M.J.N. and Park, R. (1988a), "Theoretical stress-strain model for confined concrete", *J. Struct. Div.*, ASCE, **114**, 1804-1826.
- Mander, J.B., Priestley, M.J.N. and Park, R. (1988b), "Observed stress-strain behavior of confined concrete", *J. Struct. Div.*, ASCE, **114**, 1827-1849.
- Mirmiran, A. and Shahawy, M. (1997), "Behavior of concrete columns confined by fiber composites", *J. Struct. Eng.*, ASCE, **123**, 583-590.
- Nagaya, K. and Kawashima, K. (1999), "Stress-strain model for tied reinforced concrete columns confined by carbon fiber sheets", *J. Civ. Eng.*, JSCE, **43**, 25-42.
- Newman, K. and Newman, J.B. (1971), "Failure theories and design criteria for plain concrete", *Proc. of the Int. Civil Eng. Material Conf. on Structural, Solid Mechanics, and Engineering Design*, Wiley Interscience, N.Y., 936-995.
- Park, R., Priestley, M.J.N. and Gill, W.D. (1982), "Ductility of square-confined concrete columns", *J. Struct. Div.*, ASCE, **108**, 929-950.
- Priestley, M.J.N., Seible, F. and Calvi, G.M. (1996), *Seismic Design and Retrofit of Bridges*, John Wiley & Sons Inc., N.Y.
- Richart, F.E., Brandtzaeg, A. and Brown, R.L. (1928), "A study of the failure of concrete under combined compressive stresses", Engineering Experimental Station, University of Illinois, Bulletin No. 185.
- Richart, F.E., Brandtzaeg, A. and Brown, R.L. (1929), "The failure of plain and spirally reinforced concrete in compression", Engineering Experimental Station, University of Illinois, Bulletin No. 190.
- Saatcioglu, M. and Razvi, S.R. (1992), "Strength and ductility of confined concrete", *J. Struct. Div.*, ASCE, **118**, 1590-1607.
- Sheikh, S.A. and Uzumeri, S.M. (1980), "Strength and ductility of tied concrete columns", *J. Struct. Div.*, ASCE, **106**, 1079-1102.
- Sheikh, S.A. and Uzumeri, S.M. (1982), "Analytical model for concrete confinement in tied columns", *J. Struct. Div.*, ASCE, **108**, 2703-2722.
- Wang, P. and Cheong, K.K. (2001), "RC columns strengthened by FRP under uniaxial compression", *FRP Composite in Civil Engineering*, CICE, 327-334.
- Xiao, Y. and Wu, H. (2001), "Concrete stub columns confined by various types of FRP jackets", *FRP Composite in Civil Engineering*, CICE, 293-300.

Notation

- A_{cc} : Area of core of section within center lines of perimeter spiral;
 A_e : Area of effectively confined core concrete;
 c : Cohesion of the soil or rock;
 D : Diameter of the cylinder;
 d_s : Diameter of spiral;
 E_{cf} : Elastic modulus of CFRP;
 f_c : Compressive stress of confined concrete;
 f_{cc}' : Peak compressive strength of the confined concrete;
 f_c' : Compressive strength of the unconfined concrete;
 f_l' : Effective lateral confining stress;
 f_{l1}' : Effective lateral confining strength due to stirrup;
 f_{l2}' : Effective lateral confining strength due to CFRP;
 f_{yh} : Yield strength of the transverse reinforcement;
 k_c : Coefficient of the section shape;
 k_e : Confinement effectiveness coefficient;
 α : Parameter;
 n : Jacket layers of CFRP;
 s' : Clear spacing between spiral or hoop bars;
 t : Thickness of CFRP per layer;
 ϵ_c : Axial strain of the confined concrete (compressive side is positive);
 ϵ_c' : Strain at compressive strength of the unconfined concrete f_c' ;
 ϵ_{cc}' : Compressive strain at the concrete peak strength f_{cc}' ;
 ϵ_{cf} : Ultimate strain of CFRP;
 ρ_{cc} : Ratio of area of axial steel to area of core of section;
 ρ_s : Ratio of volume of transverse confining steel to volume of confined concrete core;
 σ_1 : Axial stress;
 σ_3 : Lateral confined stress;
 ϕ : Angle of internal friction of material.